catalysts

MDPI

Supplementary Materials

Iron Carbide Nanoparticles Embedded in Edge-Rich, N and F Codoped Graphene/Carbon Nanotubes Hybrid for Oxygen Electrocatalysis

Xiaochang Qiao [1,2,*], Yijie Deng [3], Xiaochang Cao [4], Jiafeng Wu [1], Hui Guo [1], Wenhuang Xiao [1] and Shijun Liao [2,*]

[1] School of Materials Science and Engineering, Dongguan University of Technology, Dongguan 523808, China
[2] The Key Laboratory of Fuel Cell Technology of Guangdong Province, School of Chemistry and Chemical Engineering, South China University of Technology, Guangzhou 510641, China
[3] School of Resource Environmental and Safety Engineering, University of South China, Hengyang 421001, China
[4] School of Mechanical Engineering, Dongguan University of Technology, Dongguan, 523808, China
* Correspondence: qiaoxc@dgut.edu.cn(X.Q.); chsjliao@scut.edu.cn(S.L.); Tel.: +86-20-871-1358 (S.L.)

Citation: Qiao, X.; Deng, Y.; Cao, X.; Wu, J.; Guo, H.; Xiao, W.; Liao, S. Iron Carbide Nanoparticles Embedded in Edge-Rich, N and F Codoped Graphene/Carbon Nanotubes Hybrid for Oxygen Electrocatalysis. *Catalysts* **2022**, *12*, 1023. https://doi.org/10.3390/catal12091023

Academic Editors: Jose Luis Diaz de Tuesta and Helder T. Gomes

Received: 10 August 2022
Accepted: 6 September 2022
Published: 9 September 2022

Publisher's Note: MDPI stays neutral with regard to jurisdictional claims in published maps and institutional affiliations.

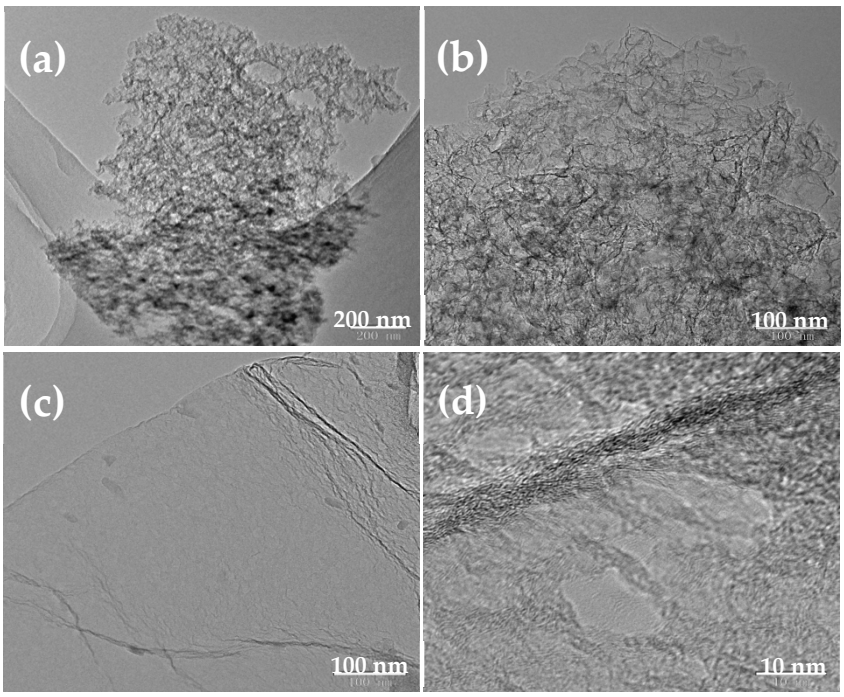

Figure S1. TEM images of Fe-F-C (a, b) and N-F-C (c, d).

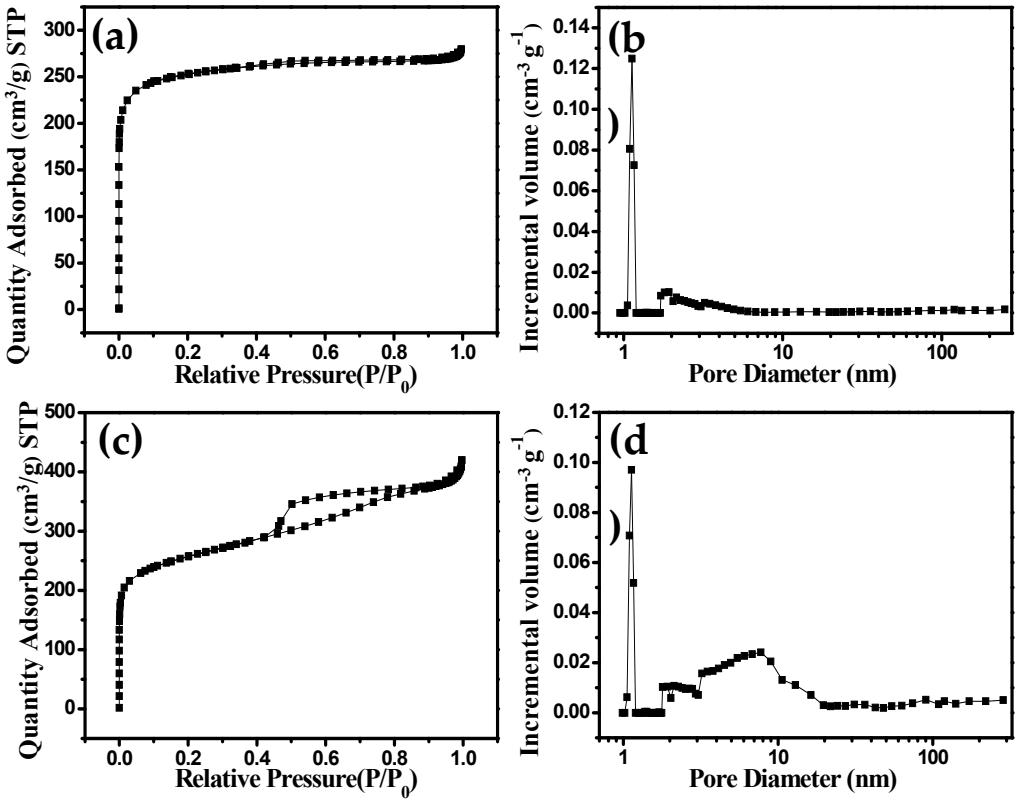

Figure S2. Nitrogen adsorption–desorption isotherms and pore-size distribution curve of N-F-C and Fe-F-C.

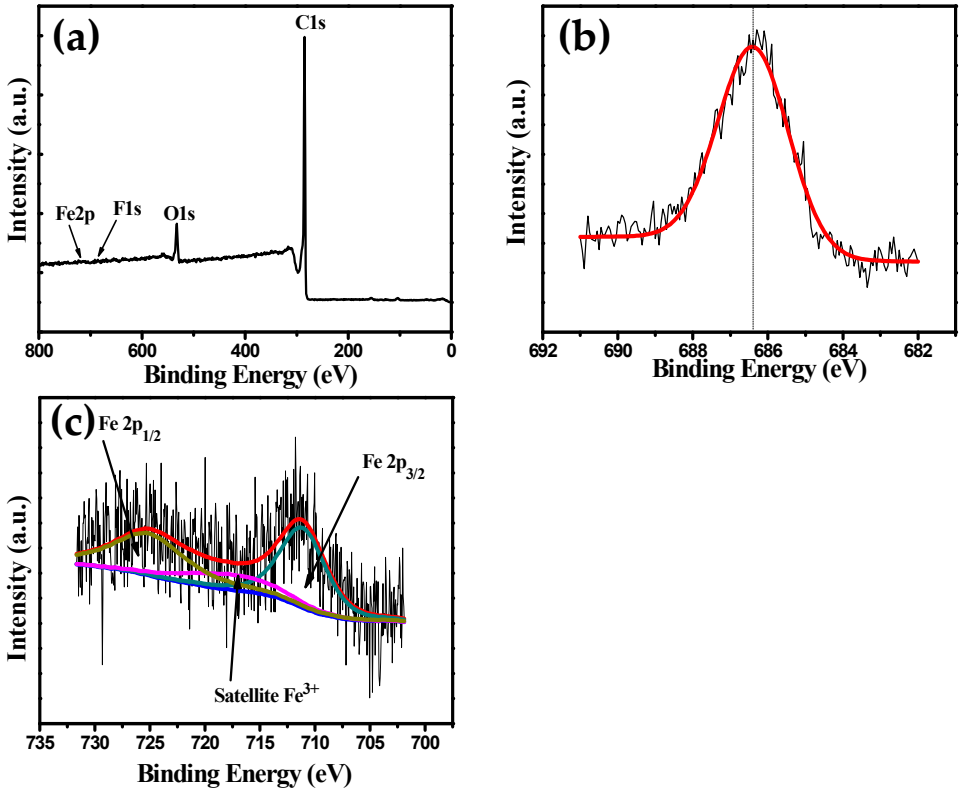

Figure S3. XPS results for Fe-F-C: survey scan (a), high resolution deconvoluted spectra for F 1s (b), and Fe 2p (c).

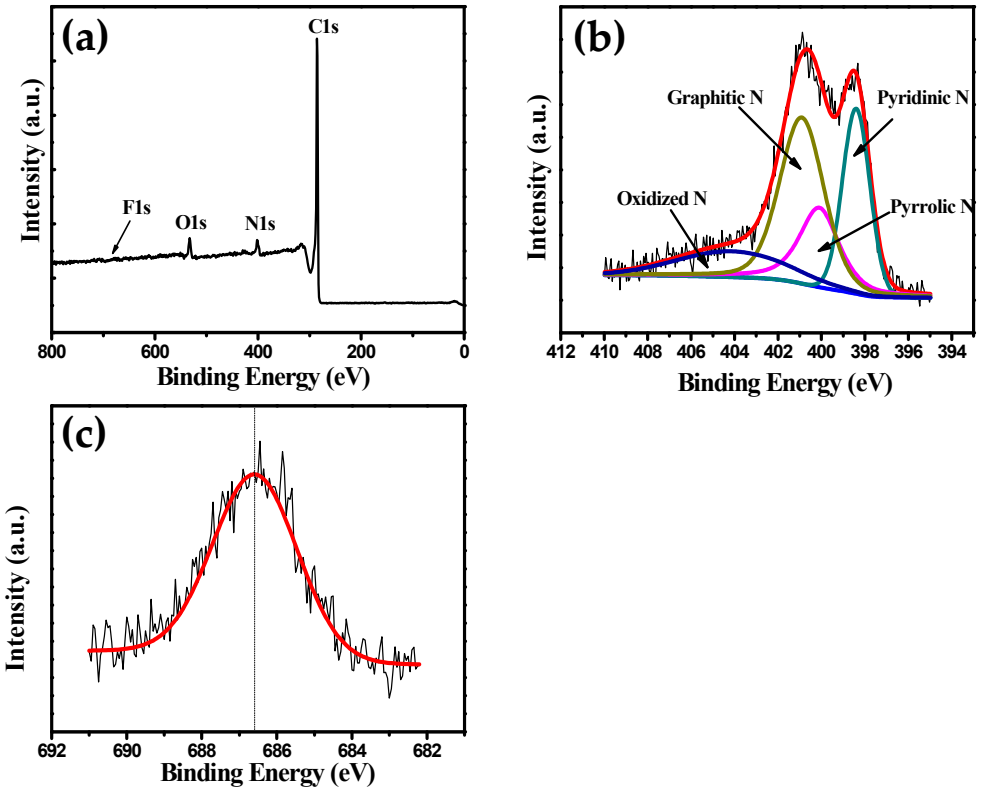

Figure S4. XPS results for N-F-C: survey scan (a), high resolution deconvoluted spectra for N 1s (b), and F 1s (c).

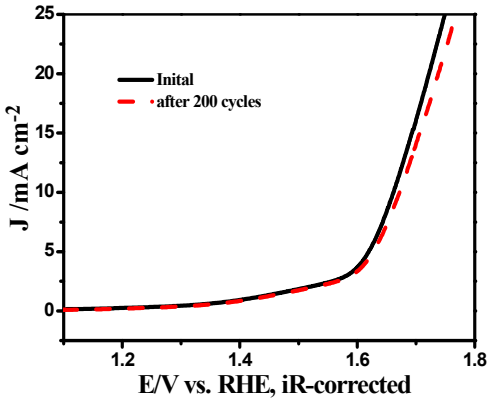

Figure S5. OER LSV plots of Fe_3C@N-F-GCNTs before and after a potential cycling of 200 cycles (c).

Table S1. Surface composition of Fe3C@N-F-GCNTs, Fe-F-C and N-F-C calculated from XPS results.

Catalyst	Species concentration (at%)				
	C	O	N	F	Fe
Fe_3C@N-F-GCNTs	91.87	3.2	3.79	0.72	0.42
Fe-F-C	91.61	7.10	–	0.90	0.39
N-F-C	89.71	3.41	6.08	0.80	–

Table S2. Distribution of each N species, obtained from the fitting results of N 1s XPS spectra (normalized to the surface N atoms of each material).

Catalyst	Species concentration (at%)			
	Pyridinic N	Pyrrolic N	Graphitic N	Oxidized N
Fe_3C@N-F-GCNTs	25.61	12.60	40.85	20.94
N-F-C	25.14	20.13	40.53	14.20

Table S3. Comparison of ORR and OER activity parameters with other recently reported highly active non-noble metal bifunctional electrocatalysts.

Catalyst	C_{KOH}	rotating rate (rpm)	$E_{J3}/E_{hafe\text{-}wave,ORR}$ (V)	$E_{J10,OER}$ (V)	$\Delta E(E_{J10,OER}\text{-}E_{J3}/E_{hafe\text{-}wave,ORR})$	Literature
Fe_3C@N-F-GCNTs	0.1 M	1600	0.846	1.662	0.816	this study
Co_9S_8@TDC-900	0.1 M	1600	0.78	1.56	0.78	[10]
S/N_Fe-27	0.1 M	1500	0.87	1.78	0.91	[36]
Fe3C@Fe,N,S-GCM	0.1 M	1600	0.779	1.557	0.778	[37]
CoMnO@CNT/CNF	0.1 M	1600	0.82	1.60	0.78	[38]
Co-N/PC@CNT	0.1 M	1600	0.78	1.63	0.86	[39]
Fe_3C@C-NGns-NCNTs	0.1 M	1600	0.855	1.642	0.787	[40]
Fe_3C@NG800-0.2	0.1 M	1600	0.81	1.59	0.78	[41]

Table S4. Comparison of the power density for Zn-air batteries.

Catalyst	Power density $mW \cdot cm^{-2}$	References
Fe_3C@N-F-GCNTs	130.0	this study
Fe-NP-WB-3	92.9	J Energy Chem 2021;55:572-579 [42]
Fe_3N@N-C	87.5	Carbon 2019;153:364-371 [43]
CoFeNi-CNTs	138.7	J Alloy Compd 2022;910 [44]
C-FeZIF-8@g-C_3N_4	121	Chem Eng J 2020;390 [45]
NDGs-800	115.2	ACS Energy Letters 2018;3(5):1183-1191 [46]
NPC-$Fe_{0.3}$	99	Chinese Chemical Letters 2022;33(4):2171-2177 [47]

Reference

1. Li, Z.; Gao, Q.; Liang, X.; Zhang, H.; Xiao, H.; Xu, P.; Liu, Z. Low content of Fe3C anchored on Fe,N,S-codoped graphene-like carbon as bifunctional electrocatalyst for oxygen reduction and oxygen evolution reactions. Carbon 2019, 150, 93-100, doi:10.1016/j.carbon.2019.05.012.
2. Zhao, J.Y.; Wang, R.; Wang, S.; Lv, Y.R.; Xu, H.; Zang, S.Q. Metal-organic framework-derived Co_9S_8 embedded in N, O and S-tridoped carbon nanomaterials as an efficient oxygen bifunctional electrocatalyst. *J. Mater. Chem. A* **2019**, *7*, 7389–7395. https://doi.org/10.1039/c8ta12116h.
3. Ranjbar Sahraie, N.; Paraknowitsch, J.P.; Göbel, C.; Thomas, A.; Strasser, P. Noble-Metal-Free Electrocatalysts with Enhanced ORR Performance by Task-Specific Functionalization of Carbon using Ionic Liquid Precursor Systems. *J. Am. Chem. Soc.* **2014**, *136*, 14486–14497. https://doi.org/10.1021/ja506553r.
4. Tian, G.L.; Zhang, Q.; Zhang, B.S.; Jin, Y.G.; Huang, J.Q.; Su, D.S.; Wei, F. Toward Full Exposure of "Active Sites": Nanocarbon Electrocatalyst with Surface Enriched Nitrogen for Superior Oxygen Reduction and Evolution Reactivity. *Adv. Funct. Mater.* **2014**, *24*, 5956–5961. https://doi.org/10.1002/adfm.201401264.
5. Ban, J.J.; Xu, G.C.; Zhang, L.; Xu, G.; Yang, L.J.; Sun, Z.P.; Jia, D.Z. Efficient Co-N/PC@CNT bifunctional electrocatalytic materials for oxygen reduction and oxygen evolution reactions based on metal-organic frameworks. *Nanoscale* **2018**, *10*, 9077–9086. https://doi.org/10.1039/c8nr01457d.
6. Qiao, X.; Jin, J.; Luo, J.; Fan, H.; Cui, L.; Wang, W.; Liu, D.; Liao, S. In-situ formation of N doped hollow graphene Nanospheres/CNTs architecture with encapsulated Fe_3C@C nanoparticles as efficient bifunctional oxygen electrocatalysts. *J. Alloy Compd.* **2020**, *828*, 154238. https://doi.org/10.1016/j.jallcom.2020.154238.
7. Xiao, J.; Chen, C.; Xi, J.; Xu, Y.; Xiao, F.; Wang, S.; Yang, S. Core–shell Co@ Co_3O_4 nanoparticle-embedded bamboo-like nitrogen-doped carbon nanotubes (BNCNTs) as a highly active electrocatalyst for the oxygen reduction reaction. *Nanoscale* **2015**, *7*, 7056–7064.
8. Li, Y.H.; Zang, K.T.; Duan, X.Z.; Luo, J.; Chen, D. Boost oxygen reduction reaction performance by tuning the active sites in Fe-N-P-C catalysts. *J. Energy Chem.* **2021**, *55*, 572–579. https://doi.org/10.1016/j.jechem.2020.07.041.
9. Li, T.F.; Li, M.; Zhang, M.R.; Li, X.; Liu, K.H.; Zhang, M.Y.; Liu, X.; Sun, D.M.; Xu, L.; Zhang, Y.W.; et al. Immobilization of Fe3N nanoparticles within N-doped carbon nanosheet frameworks as a high-efficiency electrocatalyst for oxygen reduction reaction in Zn-air batteries. *Carbon* **2019**, *153*, 364–371. https://doi.org/10.1016/j.carbon.2019.07.044.
10. Chen, D.; Li, G.F.; Chen, X.; Li, C.J.; Zhang, Y.C.; Hu, J.; Yu, J.H.; Yu, L.Y.; Dong, L.F. CoFeNi/N-codoped carbon nanotubes with small diameters derived from spherical Prussian blue analog as bifunctional oxygen electrocatalysts for rechargeable Zn-air batteries. *J. Alloy Compd.* **2022**, *910*, 164964. https://doi.org/ARTN164964,10.1016/j.jallcom.2022.164964.
11. Deng, Y.J.; Tian, X.L.; Chi, B.; Wang, Q.Y.; Ni, W.P.; Gao, Y.; Liu, Z.E.; Luo, J.M.; Lin, C.X.; Ling, L.M.; et al. Hierarchically open-porous carbon networks enriched with exclusive Fe-N-x active sites as efficient oxygen reduction catalysts towards acidic H-2-O-2 PEM fuel cell and alkaline Zn-air battery. *Chem. Eng. J.* **2020**, *390*, 124479. https://doi.org/Artn124479,10.1016/J.Cej.2020.124479.
12. Wang, Q.; Ji, Y.; Lei, Y.; Wang, Y.; Wang, Y.; Li, Y.; Wang, S. Pyridinic-N-Dominated Doped Defective Graphene as a Superior Oxygen Electrocatalyst for Ultrahigh-Energy-Density Zn–Air Batteries. *ACS Energy Lett.* **2018**, *3*, 1183–1191. https://doi.org/10.1021/acsenergylett.8b00303.
13. Yang, T.F.; Chen, Y.; Liu, Y.; Liu, X.P.; Gao, S.Y. Self-sacrificial template synthesis of Fe, N co-doped porous carbon as efficient oxygen reduction electrocatalysts towards Zn-air battery application. *Chin. Chem. Lett.* **2022**, *33*, 2171–2177. https://doi.org/10.1016/j.cclet.2021.09.014.